

Article

Optimisation of Small Hydropower Units in Water Distribution Systems by Demand Forecasting

Martin Oberascher ¹, Lukas Schartner ² and Robert Sitzenfrei ^{1,*}

¹ Unit of Environmental Engineering, Department of Infrastructure Engineering, Faculty of Engineering Sciences, University of Innsbruck, Technikerstrasse 13, 6020 Innsbruck, Austria; martin.oberascher@uibk.ac.at

² Kirchebner Ziviltechniker GmbH, Grabenweg 3a, 6020 Innsbruck, Austria; l.schartner@kirchebner.at

* Correspondence: robert.sitzenfrei@uibk.ac.at; Tel.: +43-512-507-62195

Abstract: The potential of water supply systems for renewable electrical energy production is frequently utilised by a small-scale hydropower unit (SHPU) that utilises the surplus water or pressure. However, fluctuating demand on an hourly and daily basis represents a significant challenge in operating such devices. To address this issue, a control strategy based on demand forecast is implemented, adjusting the SHPU's inflow based on current demand conditions. Thus, individual days are categorised into control categories with similar flow conditions, and control is optimised for each category using a simplified evolutionary optimisation technique. Coupled with demand forecasts, the SHPU controller evaluates on a daily basis which set of water levels to utilise for the next day to optimise energy production. This approach is implemented in an alpine municipality, and its economic feasibility is evaluated through a long-term simulation over 10 years. This approach resulted in an annual profit increase compared to the reference status based on well-informed expert knowledge. However, it is worth noting that the approach has limited suitability for further improvements within the case study. Nonetheless, SHPUs also contribute to improving water quality and, if the electrical energy generated is directly used to operate the water supply, enhance resilience to grid failures.

Keywords: control; optimisation; renewable electrical energy; water distribution network; water–energy nexus; water surplus



Citation: Oberascher, M.; Schartner, L.; Sitzenfrei, R. Optimisation of Small Hydropower Units in Water Distribution Systems by Demand Forecasting. *Water* **2023**, *15*, 3998. <https://doi.org/10.3390/w15223998>

Academic Editor: Stefano Alvisi

Received: 13 October 2023

Revised: 14 November 2023

Accepted: 15 November 2023

Published: 17 November 2023



Copyright: © 2023 by the authors. Licensee MDPI, Basel, Switzerland. This article is an open access article distributed under the terms and conditions of the Creative Commons Attribution (CC BY) license (<https://creativecommons.org/licenses/by/4.0/>).

1. Introduction

The sustainable development and operation of water supply systems require the involvement of the water–energy nexus, as these complex systems exhibit high interdependence [1–3]. For instance, energy is required for the abstraction, treatment, and distribution of drinking water in water supply systems, contributing to 3% of the total electricity consumption and 1% of greenhouse gas emissions [2,4].

In this context, the potential of water distribution networks as a source of renewable electrical energy is increasingly recognised [5,6]. A decentralised and small-scale hydropower unit (SHPU) is installed to utilise the surplus pressure and/or inflow between elevation tanks and lower-lying supply areas for electricity generation. Consequently, SHPUs provide a viable alternative to pressure reduction valves for energy dissipation [7]. These units can be implemented using traditional machines, such as Francis, Pelton, or crossflow turbines, or adapted machines, such as pumps, as turbines or tubular propellers designed specifically for water supply purposes [8]. Global assessments of the potential and economic feasibility of SHPUs have been conducted worldwide, including Austria [9], Brazil [10], Italy [11,12], Iran [13–15], Israel [16], Portugal [17,18], South Africa [19], and Switzerland [20]. As the literature shows, the generated electrical energy is, thereby, strongly influenced by the location of the SHPU [9,21–23], and therefore, the spatial positioning of these devices represents an important criterion for installation.

However, a significant challenge in operating such devices arises from a highly variable environment characterised by daily and hourly fluctuations in water demand and absolute prioritisation of demand coverage. Consequently, the availability of water and pressure surpluses changes rapidly. One potential solution proposed by Monteiro, Delgado, and Covas [18] and Brady, et al. [24] is the implementation of two or more SHPUs in parallel to maximise electrical energy production during periods of high variability in water flow and pressure. Additionally, to structural measures, the real-time control of SHPUs represents another innovative approach to address these fluctuations by considering current system states [25–28].

To tackle this challenge, Sitzenfrei and von Leon [29] introduced a simple control strategy based on the filling depth of storage tanks to increase electrical energy production. Three operating levels, corresponding to specific depths in the tank, were defined, and their heights were determined based on expert knowledge. In a subsequent study, Sitzenfrei, et al. [30] investigated the effectiveness of different parameter sets for these operating levels by optimising them with an evolutionary algorithm and long-term simulation of the water supply system. However, optimising the three operating levels showed minimal improvement due to the highly volatile input involved in optimising 365 different daily consumption cycles.

The above-described real-time control strategies are based on current system conditions; to the best of the authors' knowledge, the potential of demand forecasts to optimise the electrical energy production of SHPUs has not been investigated in detail so far. Therefore, this study proposes that water consumption correlates with various external parameters (e.g., the day of the week), enabling prediction of the next day's water consumption. By optimising the SHPU control for a smaller input set, e.g., only the highest and lowest water demand days of the year, it is assumed that more suitable water levels can be obtained, leading to increased electrical energy production. With the aid of a daily forecast, the SHPU controller can then reassess and determine the optimal water levels for the following day to maximise electrical energy production.

2. Materials and Methods

The control strategy developed by Sitzenfrei and von Leon [29] is designed to optimise the operation of a small-scale hydropower unit (SHPU) in a water distribution network characterised by a highly variable environment (e.g., daily fluctuations in water consumption, flow, and pressure conditions). This strategy is to maximise the utilisation of surplus water for electrical energy production while ensuring a consistent water supply. The controller is implemented as a rule-based controller by adjusting the nozzle area of a Pelton turbine based on the current water level in the storage tank.

Figure 1 provides an overview of the developed control strategy. There are three defined water levels in the storage tank (H_1 , H_2 , and H_3), which serve as operating levels for control actions:

- Maximum flow operation: When the storage tank is approximately full and the water level is above H_2 , the SHPU operates at maximum flow.
- Normal flow operation: When the water level is between H_1 and H_2 , the turbine operates with the current settings.
- Flow reduction: If the water level falls between H_1 and H_3 , the control strategy involves gradually reducing the turbine's flow rate by 1/8 of the maximum flow rate. This reduction in flow rate aims to restore the water level in the subsequent simulation time step. However, if the water level in the storage tank continues to decrease despite the flow rate reduction, the turbine's flow rate is further reduced.
- SHPU shutdown: If the water level falls below H_3 , the control strategy involves completely shutting off the turbine to ensure an adequate water supply is reserved for firefighting.
- Resuming maximum flow operation: Once the water level rises above H_2 again, the control strategy sets the turbine back to maximum flow.

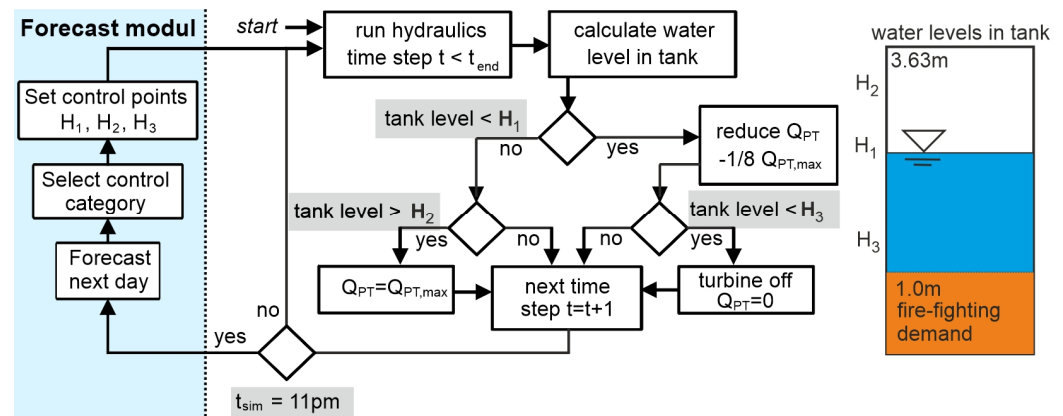


Figure 1. Overview of the control strategy reused from [29] and [30] with permission from Elsevier, whereby the demand and spring forecasting as an extension of this work is highlighted in colour.

As mentioned in the introduction, the objective of this work is to further enhance the operation and increase the amount of energy generated by incorporating forecasts for the next day into the control strategy. To achieve this, the aforementioned control strategies are extended with an additional control rule (highlighted in colour in Figure 1), which is executed at 11 pm for the following day. Forecasts are made for water availability and total water demand, and based on these predictions, the control category for the next day is selected. Subsequently, the operating levels H_1 , H_2 , and H_3 are determined through a previously optimised process for each control category. A detailed explanation of this procedure is provided in the following subchapter.

2.1. Optimisation of the Control Strategy

2.1.1. Control Categories

The objective of the control categories is to classify the input data (e.g., water availability and demand) into groups, where the values within each category exhibit similar flow conditions. These control categories aim to provide optimal input sets for prediction and the enhancement of electrical energy production. Therefore, statistical evaluations of water availability and demand are carried out, and based on that, these data are categorised into different control categories. In this work, one and six control categories are chosen for comparison (for more information on the control categories, refer to the corresponding subchapter in the results section).

2.1.2. Optimisation of Operating Levels

After defining the control categories, the operating levels H_1 , H_2 , and H_3 are optimised for each category. The aim of this process is to maximise electrical energy production by determining the optimal operating levels using a simplified evolutionary optimisation technique, where the next generation is created with a Monte Carlo sampling technique [31] within the best solutions of the previous generation. Thereby, the best solutions are selected based on the electrical energy generation, and the operation levels H_1 , H_2 , and H_3 are determined. In the next step, the operation levels for the offspring are randomly selected between these values, meaning that all H_1 of the new generation are between $H_{1,min}$ and $H_{1,max}$ of the previous generation. The simplified evolutionary optimisation technique is developed and described in more detail in Sitzenfrie and Rauch [32], whereas in the following, the process is briefly explained.

In the first step, value ranges are established for each operating level based on the physical limits imposed by the storage tank’s geometry. Dependencies among the operating levels, such as the requirement for H_2 to be greater than H_1 and H_1 to be greater than H_3 , are defined, and random values are assigned to them. Specifically, H_1 is selected randomly within the range of 1.5 m and 3.5 m using a uniform distribution. Next, H_2 is chosen

randomly between H_1 and the maximum water level of the storage tank. H_3 is selected randomly between the minimum water level in the storage tank and 2.5 m using a uniform distribution. If H_3 is larger than H_1 , H_3 is set to H_1 minus 0.1 m.

In the second step, 100 different sets of operating level triples are generated, conducting a long-term simulation for each set to calculate the electrical energy produced. For the long-term simulation, the same numerical model of the case study (for more information, refer to Section 2.3.2) is applied. The simulation period corresponds to the number of days within the corresponding control category. This assumption neglects certain dynamics of inflow and demands over a longer period. However, inflows and demands are, in general, quite similar over the longer term (for more information, refer to Section 2.3.1), and changes in other control categories occur less frequently than days with similar values.

Subsequently, the top 10% of triples with the highest energy production are further evaluated based on their operating levels. In the second generation, 100 new random triples are generated, but the values of H_1 , H_2 , and H_3 are restricted to fall within the range of the previous best 10%. If any random selection violates the defined dependencies, the values are adjusted to be 0.01 m below or above the neighbouring level. This process is repeated for each subsequent generation, resulting in the convergence of the operating levels towards their respective optima for maximum electrical energy production.

Due to the rapid convergence of the applied method [32], the maximum number of generations is set to 10. Furthermore, two stopping criteria are defined to reduce the optimisation process runtime in the case of minor changes. The optimisation process stops when either the differences in electrical energy production among the 100 different triples are less than 100 kWh or the differences between each operating level are less than 0.1 m. Additionally, it is evaluated that the availability of sufficient water and hydraulic heads meet the required water demand within the network throughout the entire investigation period. The water pressure is assessed at three control nodes, and if the hydraulic head falls below a specified threshold, the corresponding triple is removed from further consideration.

2.1.3. Forecasting of Control Categories

After optimising the individual control categories, the optimal operating levels for operating the SHPU for the next day are determined for each category. At 11 p.m., the future spring discharge and total water demand for the case study scheduled for the following day are forecasted. The day is subsequently categorised into one of the six control categories. The optimal operating levels for this specific category are then retrieved and integrated into the turbine's control. The following forecasting approaches are investigated:

- Perfect forecast: Assumes a perfect forecast where the predicted control categories match the actual conditions with 100% accuracy, representing the maximum potential of the forecast.
- Tomorrow like today: Assumes that the spring discharge and total water demand will be the same as the current day.
- Tomorrow like last week: Assumes that the spring discharge and total water demand will be the same as the corresponding weekday last week.
- False forecast: Examines the effect of an incorrect forecast as the worst-case performance scenario. The correct control category is disregarded, and the control category for the next day is randomly selected from the remaining categories.

2.2. Profitability Analysis

For comparison, the yearly profit is determined by subtracting operational and capital costs from the benefit. Therefore, the calculation of Sitzenfrei and von Leon [29] is adopted, which can be summarised as follows.

In the first step, the yearly benefit B (€/a) is determined with Equations (1) and (2):

$$EP = \frac{1}{1000} * \sum_{t=0}^{tsim} * \eta_G * \eta_{T,t} * Q_t * H_t * \rho * g * t \quad (1)$$

$$B = \frac{ET * p}{t_{sim}} \quad (2)$$

in which EP is the energy production (kWh), η_G is the efficiency of the generator and other plant components (-), $\eta_{T,t}$ is the efficiency of the Pelton turbine (-), Q_t is the flow (m^3/s), H_T is the hydraulic head (m) at the installation place of the Pelton turbine, ρ is the density of water (kg/m^3), g is the earth acceleration (m/s^2), t is the simulation time step (h), t_{sim} is the total simulation period (a), and p is the energy tariff ($\text{€}/kWh$).

The total investment costs I (€) are calculated as follows:

$$I = I_{Pelton} * DP + I_{Additional} \quad (3)$$

in which I_{Pelton} is the investment costs for the SHPU ($\text{€}/kW$), DP is the design performance, and $I_{Additional}$ is the additional costs for installation. Based on the investment costs, the operational costs OC ($\text{€}/a$) and capital costs CC ($\text{€}/a$) are estimated with Equations (4) and (5):

$$OP = 0.03 * I \quad (4)$$

$$CC = AF * I \quad (5)$$

in which AF is the annuity factor (-). Finally, the profit per year is determined with the following equation:

$$Profit = B - OP - CC \quad (6)$$

2.3. Case Study

The case study is a water distribution network of an alpine municipality in Austria supplying 2.500 inhabitants. The network includes a storage tank with a capacity of $1.440 m^3$ to balance daily water fluctuations and to provide the necessary demand for firefighting. The storage tank is filled by a hillside spring, and it is positioned approximately 30 to 90 m above the supply area (Figure 2). The water distribution network is fully gravity driven, ensuring sufficient hydraulic pressures even during peak flow periods. For security reasons, the real layout is not depicted here in Euclidean space; instead, a distorting function from NetworkX [33] is utilised for illustration.

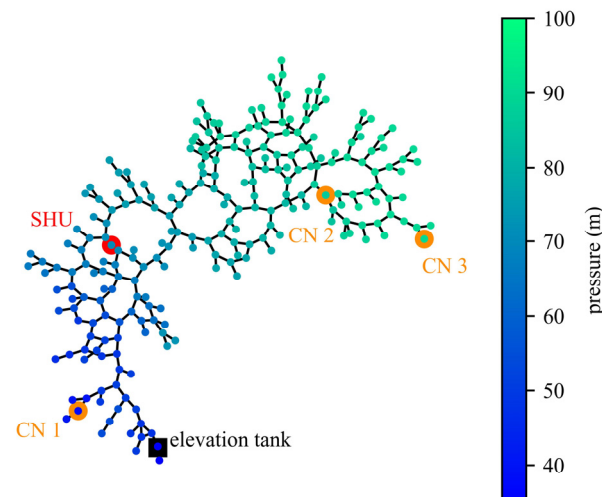


Figure 2. The hydraulic model showing the pressure at maximum flow according to [20]. The position of the hydropower station and the control points are highlighted with red and orange circles.

2.3.1. Water Surplus

For the case study, the data on inflow and outflow of the storage tank are available at a daily resolution over a 10-year period from 2003 to 2012. These data correspond to both the spring discharge and the total water demand of the case study, respectively. As

shown in Figure 3a, the spring exhibits significant fluctuations with higher levels observed during the spring and summer months and lower levels in winter. On average, the spring discharge is $1.180 \text{ m}^3/\text{day}$. Similarly, total water demand experiences seasonal variations throughout the year with peak demand occurring during the summer due to irrigation. The average daily total water demand is approximately $704 \text{ m}^3/\text{day}$. The difference between the spring discharge and total water demand, which is represented by the grey area in Figure 3a, results in a water surplus. The water surplus has an average value of $476 \text{ m}^3/\text{day}$. For more information, Figure 3b provides the cumulative distribution function of the water surplus over the investigation period. Currently, the water surplus is discharged into a nearby receiving water in close proximity to the tank. However, there is the potential to utilise the water surplus for the implementation of an SHPU and discharge it further downstream to the receiving water, thereby utilising the additional height difference for energy production.

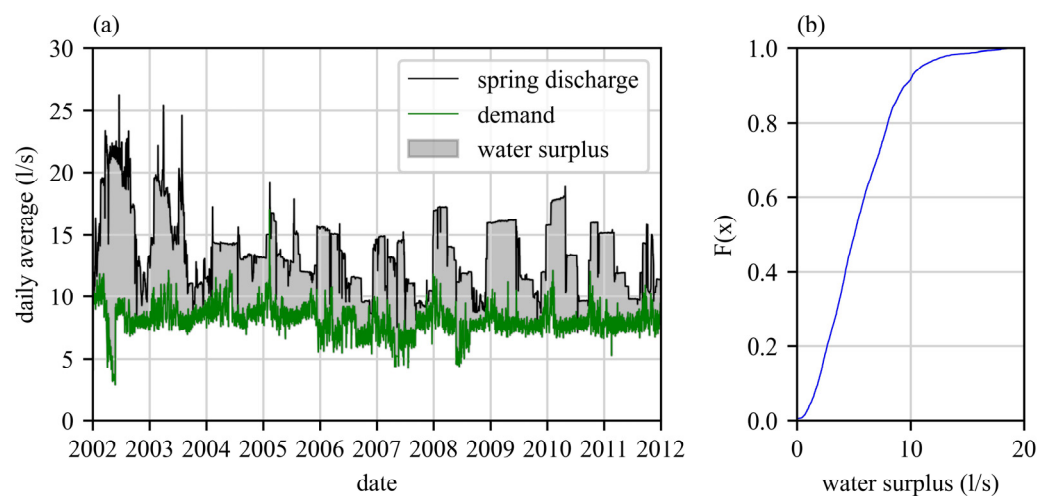


Figure 3. (a) Daily spring discharge and total water demand of the case study over the investigation period according to [21] and (b) cumulative distribution function of the water surplus usable for the SHPU.

2.3.2. Numerical Model

The analysis employs a calibrated numerical model described in [29], consisting of 243 nodes and 269 pipes, and is implemented in EPANET 2.2 [34]. The Python EPANET toolkit provided by Open Water Analytics (<https://github.com/OpenWaterAnalytics/epanet-python/tree/dev/epanet-module>, accessed on 14 August 2019) is applied for the extended period simulation covering the 10-year timeframe. The simulation accounts for water demand fluctuations by incorporating hourly and daily patterns derived from the empirical data. Additionally, three control nodes (marked as orange circles in Figure 2) are selected to ensure a minimum hydraulic head is always maintained. As the actual one-time minimum pressure without an SHPU in the network is approximately 21 m, the limit is set at 20 m, capturing significant deteriorations in the system without falsely eliminating the actual state. Further details on the case study can be found in [29].

2.3.3. Small Hydropower Unit

The SHPU is implemented in the EPANET model as a Pelton turbine, and its modelling involves setting the emitter coefficient during simulation. The optimal location for the SHPU (marked as a red circle in Figure 2) and its design performance of 3 kW were determined by Sitzenfrei and von Leon [29] and Sitzenfrei, von Leon, and Rauch [30]. These parameters are adopted in this work.

For the profitability analysis, assumptions from [29] are used for comparison: the generator efficiency η_G is assumed to be 0.95, and the device efficiency curve for the selected Pelton turbine is shown in Figure 4. The energy tariff is 0.1055 €/kWh , while the investment

costs for the Pelton turbine and the additional expenses are assumed to be 3123 €/kW and 11,000 €, respectively. Furthermore, an annuity factor of 0.084 is applied, assuming an amortisation period of 15 years and a real interest rate of 3%.

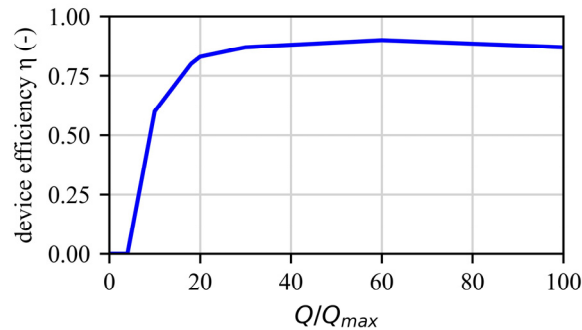


Figure 4. The device efficiency curve for the considered Pelton turbine with a design performance of 3 kW according to [20].

3. Results and Discussion

3.1. Optimisation with One Control Category

The optimisation is first carried out with one control category. Subsequently, the optimal operating levels are determined for the whole dataset, including water availability and demand (no further subdivision). Figure 5 illustrates the convergence of the 100 sets of operating levels across generations towards the optimal configuration for achieving the highest possible electrical energy production. The boxplot represents the range of profits achieved in the different generations, while the line plots display the depth in the storage tank for the three operating levels. In this case, it took only seven generations out of a maximum of ten to reach a stable state with minimal changes in the produced electrical energy and ranges of the operating levels. Despite the wide range of annual profits and operating levels in the second generation, the profits are already close to the optimum.

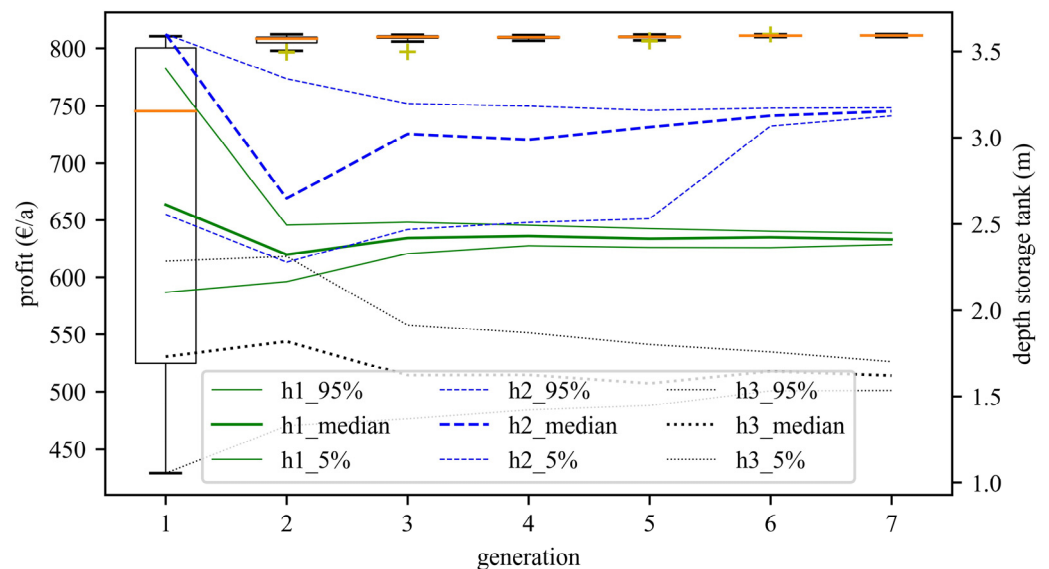


Figure 5. Convergence of the optimisation algorithm.

The robustness of the solution is further demonstrated in Figure 6, which showcases the relationships between annual profit and the magnitude of the operating levels for the best 100 solutions. The blue markers represent the operating levels of the reference scenario based on the empirical data. The x-axis is fixed according to the possible depths in the storage tank: h_1 ranges from 1.5 to 3.5 m, h_2 ranges from 1.5 to 3.63 m, and h_3 ranges from 1.0 to 2.5 m. As observed in Figure 6b,c, a relatively high profit can be achieved

without precise knowledge of the optimal ranges for H_2 and H_3 . In contrast, H_1 shows a tighter clustering of profitable settings between 2.0 and 2.7 m (Figure 6a) compared to the broader range of values for H_2 and H_3 . Consequently, the selection of the filling depth from where the turbine inflow is gradually reduced has a greater impact on the results than the switch-off point or the switch-on point after water level regeneration.

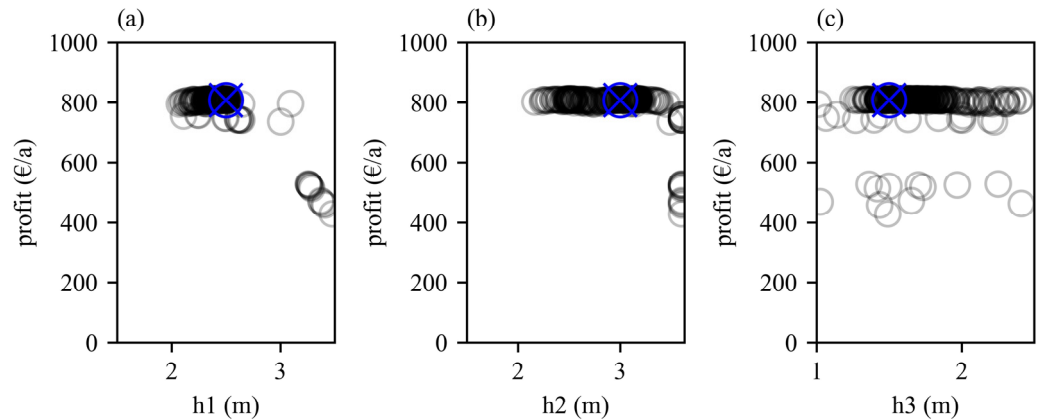


Figure 6. Annual profits depending on different parameter settings of the TWKW control system in comparison with the reference scenario (blue markers).

3.2. Optimisation with Six Control Categories

In this chapter, water availability and demand are categorised into six control categories to achieve better control conditions. Subsequently, the operating levels are optimised within this control category, resulting in a total of 18 optimised operating levels for the whole dataset.

Therefore, the daily spring discharge and total water demand from the case study are used to classify the data into six control categories. First, the daily water demand is divided into three consumption categories based on the 33.33 and 66.67% percentiles. Since the daily water demand over the 10-year period follows a normal distribution (as shown in Figure 7), the values in the middle third are more concentrated, while the values in the outer thirds cover a wider range, including outliers.

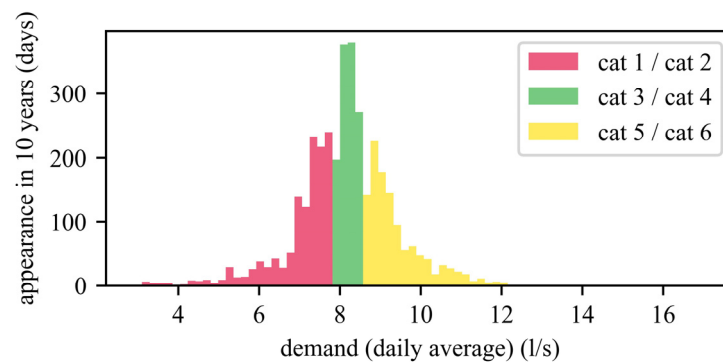


Figure 7. Distribution of total water demand from 10 years with a subdivision into the corresponding control category.

Next, the spring discharges associated with daily consumption are considered for each consumption category. By calculating the median of these inflows, the items within a consumption category can be divided into two final categories that represent the upper and lower halves of the inflows along with their associated consumptions. As a result, the control categories are classified as follows:

- Category 1: Low water demand with low spring discharge;
- Category 2: Low water demand with high spring discharge;

- Category 3: Medium water demand with low spring discharge;
- Category 4: Medium water demand with high spring discharge;
- Category 5: High water demand with low spring discharge;
- Category 6: High water demand with high spring discharge.

Figure 8 provides additional information by displaying the range of daily spring discharge (inflow) and total water demand (demand) for each control category as coloured light blue and light red boxes, respectively (secondary y -axis). Thereby, the average daily inflow is between 13 and 16 L/s for high spring discharge (categories 2, 4, and 6) and between 4 and 14 L/s for low spring discharge (categories 1, 3, and 5). In contrast, the water demand is between 3 and 7.5 L/s for low water demand (categories 1 and 2), between 7.5 and 8.5 L/s for medium water demand (categories 3 and 4), and between 8.5 and 17.0 L/s for high water demand (categories 5 and 6). As the water demand is roughly normally distributed, the range for water consumption for the medium water demand is relatively narrow compared with other categories. Additionally, the optimisation results for the three operating levels are represented as boxplots for each control category, indicated by green, blue, and black colours for H_1 , H_2 , and H_3 , respectively (primary y -axis). The boxplots show the results of the best 100 different triples, whereas the values for H_1 vary between 1.55 and 3.25 m, for H_2 vary between 2.10 and 3.30 m, and for H_3 vary between 1.05 and 2.10 m within these triples. For more details, the correlations of the different operating levels for the best 100 results per category are illustrated in Figure 9. Figure 9a for H_1 and H_2 ; Figure 9b for H_1 and H_3 ; and Figure 9c for H_2 and H_3 .

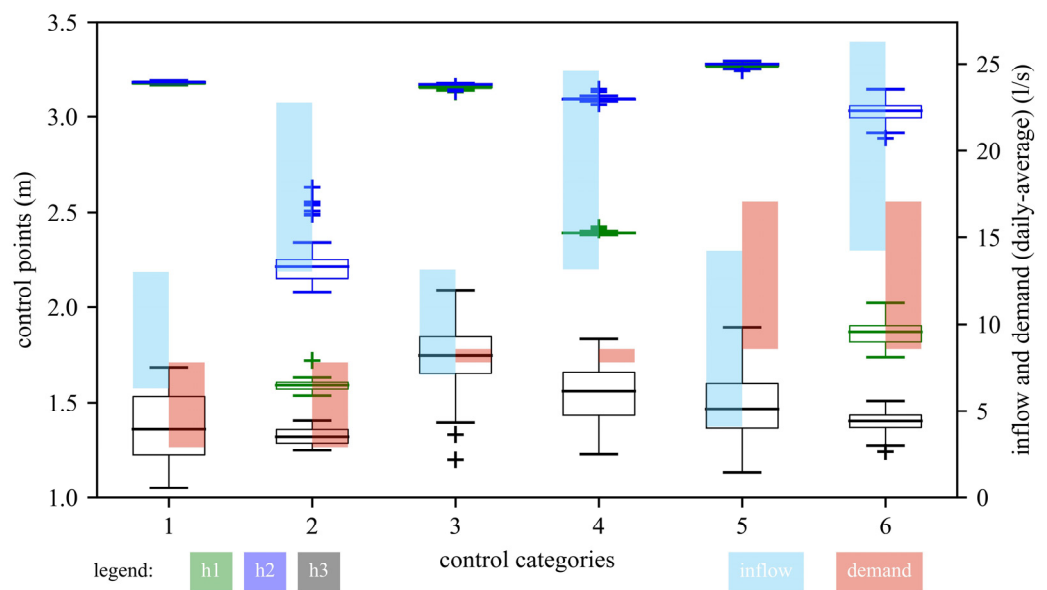


Figure 8. Results of the optimisation of the operating levels H_1 (green), H_2 (blue), and H_3 (black) in comparison with the spring discharge (inflow, light blue) and total water demand (demand, light red) for the six control categories.

As can be concluded, there is a clear difference in the performance of the SHPU under high and low spring discharges in Figures 8 and 9. Interestingly, H_1 has the highest values in the categories 1, 3, and 5, which are associated with a low discharge flow, and is just below the operating level H_2 . This indicates that the SHPU flow is reduced very early within these categories, and it is mainly operated with a reduced flow rate to achieve the highest electrical energy production. Furthermore, there is no correlation between H_3 and H_1 or H_2 for these categories, and the switch-off point (H_3) has a strong variation between the optimised trigger level, showing no correlation to the other two operating levels, H_1 and H_2 .

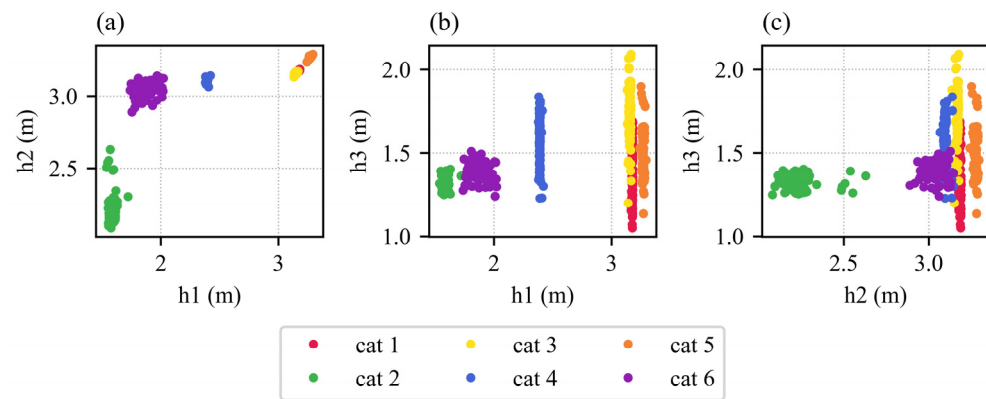


Figure 9. Correlations of the different water level heights of the best 100 results of the optimisation for each of the 6 categories.

In contrast, the ranges of H_1 and H_2 for the top 100 solutions are clearly distinguishable for high spring discharge (categories 2, 4, and 6). For example, category 2, representing optimal turbine operation with a low water demand and high spring discharge, has the lowest values for all three operating levels. The turbine operates at maximum flow already at a water level of 2.2 m (H_2), whereas the turbine flow is continuously reduced only below a water level of approximately 1.6 m (H_1). Therefore, the influence of the two operating levels H_1 and H_2 on the switch-off point is small, as H_3 shows a small bandwidth.

Additionally, the optimisation results for most categories show the widest range for H_3 among the three operating levels. This suggests that the operating levels for reduction (H_1) and full load (H_2) have a greater impact on the produced electrical energy than the switch-off point H_3 .

3.3. Economic Evaluation

For the economic evaluation, a total of five scenarios were considered and compared to the reference state of Sitzenfrei and von Leon [29], who implemented the control system based on empirical knowledge. Table 1 provides an overview of the simulation results, comparing the annual profit changes relative to the reference state, which had an annual profit of 807.64 €. In the first scenario, with a single category and no forecast, the operating levels were optimised, and the annual profit was increased to 812.42 €, corresponding to a 0.6% increase. Furthermore, using a perfect forecast with six control categories led to a profit increase of +1.1% or approximately 9 € compared to the reference state. Implementing six control categories with the forecast “tomorrow as today” (assuming tomorrow to be identical as today) or “tomorrow as last week” (assuming tomorrow to be identical to the same day of the previous week) resulted in an increase of 1.1% and 0.9%, respectively. Interestingly, even with a completely incorrect forecast, the annual profit only decreased by −3.1% to approximately 783 €.

Table 1. Results of different scenarios.

Scenario	Profit (€/a)	Change (%)
Reference state ¹	807.64	-
One category—Without forecast	812.42	+0.6
Six categories—Perfect forecast	816.78	+1.1
Six categories—Tomorrow as today	816.19	+0.9
Six categories—Tomorrow as last week	811.31	+0.5
Six categories—False forecast	782.65	−3.1

Note: ¹ The profit of the SHPU with operating levels based on local experiences and without forecast [20] was assumed to be the reference state.

3.4. Limitations and Future Research Directions

Based on the simulation results, it can be concluded that, even using an unrealistically “perfect” forecast, the increases in electrical energy production and annual profit are only marginal. The optimisation performed with the previous control categorisation and a perfect forecast showed a yearly profit increase of +1.0%, approximately twice as high as the optimisation without categorisation (+0.59%). However, considering the effort required to implement advanced control strategies (e.g., data acquisition, modelling, optimisation, prediction, and the corresponding design and operation of the SHPU), an additional annual profit of +9 €/a (+1.1%) appears to be minimal. Nevertheless, the proposed control scheme with the operating levels was found to be very robust in terms of maximising electrical energy production.

Therefore, further improvements and optimisation of the control strategy compared to the reference state with well-chosen expert values are only partially suitable for this case study. However, from the authors’ perspective, a prediction model could be useful if the efficiency curve deviates from the plateau-like shape used in this work or if other (temporal) aspects are considered, which could be addressed in future research. For example, if a pump as turbine (PAT) with a steep and narrow device efficiency curve is used, larger increases in efficiency can be expected from the optimisation process. Furthermore, an application potential is observed with a fluctuation in electricity prices, allowing for temporally optimised electrical energy generation at high feed-in tariffs. Additionally, prediction models could be applied to coordinate the operation of multiple installed SHPUs by optimising their operating times. However, due to the design of elevation tanks as daily balance tanks with a required fire-fighting water reserve, considering an optimisation over multiple days appears to be less effective.

3.5. Further Discussion

A positive side-effect of implementing an SHPU is the improvement of water quality. The increased water demand due to the SHPU reduces the residence time of water in the network, resulting in a positive effect on water quality in (parts of) the network. Figure 10 presents a comparison of water age at the three control nodes located throughout the network. As shown, the SHPU can reduce the peak water age by up to 72 h at the beginning of the investigation period. On average, a reduction of approximately 24 h in water age is achieved in the long-term.

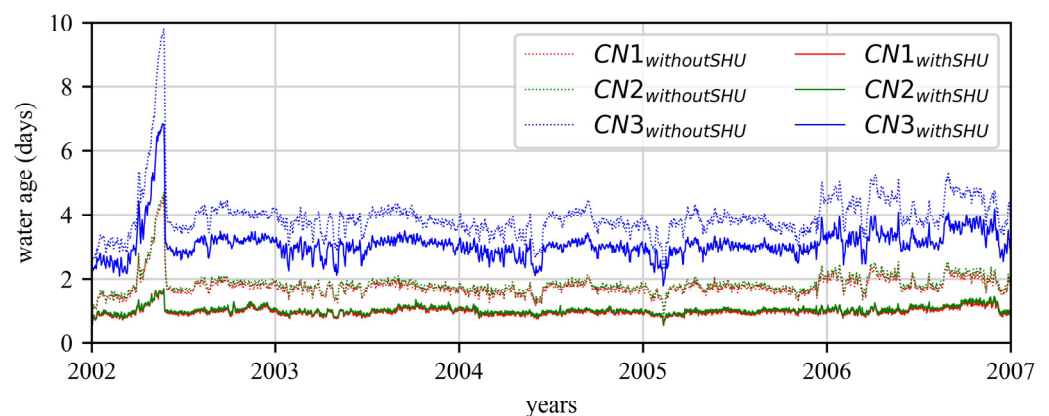


Figure 10. Comparison of the water age for the three control nodes with and without an SHPU.

Additionally, disturbances in water and energy networks are closely interconnected. For example, a power grid outage can lead to pump or treatment plant failures, potentially resulting in emergency operations in the water supply system. A water distribution network typically consists of different pressure zones that require a pressure increase or reduction depending on topological conditions. Additionally, water can be sourced from groundwater wells or higher altitude sources. If the energy generated with an SHPU is directly used

by the operators (e.g., for a treatment after the SHPU or to direct it to a low-pressure zone to increase pressure [16]), it can further enhance the resilience of water supply systems. This application potential is particularly significant in mountainous regions like the alpine area due to greater altitude differences. Furthermore, these findings will be integrated into our current research project 'RESIST', where the aim is to improve the resilience of water distribution systems against multiple failures, including a power outage.

4. Conclusions

A small hydropower unit (SHPU) installed in a water distribution network operates in a highly variable environment characterised by pressure and demand fluctuations over short periods, which can impact their electrical energy production. Sitzenfrei and von Leon [20] developed a simple control strategy to adjust the inflow to the SHPU based on the water level in the storage tank. However, further optimisation of the control strategy did not yield significant improvements due to the highly volatile input into the optimisation task [21].

In this work, demand forecasts are integrated into the control strategy to address this limitation, and the optimisation potential for electrical energy generation is evaluated. Therefore, input data, such as water availability and demand, were categorised based on similar flow conditions. Subsequently, the SHPU control was optimised for each control category to obtain more suitable operating levels for different system conditions. The operating levels were optimised using a simplified evolutionary optimisation technique developed by Sitzenfrei and Rauch [32], where the next generation is created with a Monte Carlo sampling technique within the best solutions of the previous generation. The SHPU controller was integrated with various types of daily forecast to predict the category of the next day and to set optimal water levels to further enhance the electrical energy potential. The implementation of the SHPU was carried out in an alpine municipality, and the economic feasibility was evaluated through a 10-year long simulation. The main conclusions drawn from the obtained results are as follows:

- Incorporating demand forecasts and adjusting controls for different flow conditions can improve the electrical energy potential of an SHPU;
- However, it is worth noting that the controls in the reference state were already based on well-reasoned expert knowledge, making improvements marginal compared to the effort required for more complex control strategies in this specific case study;
- The prediction approach shows potential when dealing with devices that have a steep and narrow device efficiency curve, such as pump as turbines, or when considering fluctuating electricity prices;
- Additionally, an SHPU can significantly improve the quality of drinking water due to higher abstraction volumes, and if the generated electrical energy is directly used to operate the network, it also increases the resilience of the water supply system against outages of the power grid.

Author Contributions: Conceptualisation and methodology, L.S. and R.S.; software, L.S. and M.O.; writing—original draft preparation, L.S. and M.O.; writing—review and editing, R.S. All authors have read and agreed to the published version of the manuscript.

Funding: The project "RESIST" is funded by the Austrian security research programme KIRAS of the Federal Ministry of Finance (BMF).

Data Availability Statement: The data presented in this study are available on request from the corresponding author. The data are not publicly available due to security reasons (critical infrastructure).

Conflicts of Interest: Author Lukas Schartner was employed by the company Kirchebner Ziviltechniker GmbH. The remaining authors declare that the research was conducted in the absence of any commercial or financial relationships that could be construed as a potential conflict of interest.

References

1. Lee, M.; Keller, A.A.; Chiang, P.-C.; Den, W.; Wang, H.; Hou, C.-H.; Wu, J.; Wang, X.; Yan, J. Water-energy nexus for urban water systems: A comparative review on energy intensity and environmental impacts in relation to global water risks. *Appl. Energy* **2017**, *205*, 589–601. [\[CrossRef\]](#)
2. Vakilifard, N.; Anda, M.; Bahri, A.P.; Ho, G. The role of water-energy nexus in optimising water supply systems—Review of techniques and approaches. *Renew. Sust. Energ. Rev.* **2018**, *82*, 1424–1432. [\[CrossRef\]](#)
3. Wu, W.; Maier, H.R.; Dandy, G.C.; Arora, M.; Castelletti, A. The changing nature of the water–energy nexus in urban water supply systems: A critical review of changes and responses. *J. Water Clim. Chang.* **2020**, *11*, 1095–1122. [\[CrossRef\]](#)
4. Rothausen, S.G.S.A.; Conway, D. Greenhouse-gas emissions from energy use in the water sector. *Nat. Clim. Chang.* **2011**, *1*, 210–219. [\[CrossRef\]](#)
5. Sari, M.A.; Badruzzaman, M.; Cherchi, C.; Swindle, M.; Ajami, N.; Jacangelo, J.G. Recent innovations and trends in in-conduit hydropower technologies and their applications in water distribution systems. *J. Environ. Manag.* **2018**, *228*, 416–428. [\[CrossRef\]](#)
6. Giudicianni, C.; Mitrovic, D.; Wu, W.; Ferrarese, G.; Pugliese, F.; Fernández-García, I.; Campisano, A.; De Paola, F.; Malavasi, S.; Maier, H.R.; et al. Energy recovery strategies in water distribution networks: Literature review and future directions in the net-zero transition. *Urban Water J.* **2023**, 1–16. [\[CrossRef\]](#)
7. Creaco, E.; Campisano, A.; Fontana, N.; Marini, G.; Page, P.R.; Walski, T. Real time control of water distribution networks: A state-of-the-art review. *Water Res.* **2019**, *161*, 517–530. [\[CrossRef\]](#)
8. Pérez-Sánchez, M.; Sánchez-Romero, F.; Ramos, H.; López-Jiménez, P. Energy Recovery in Existing Water Networks: Towards Greater Sustainability. *Water* **2017**, *9*, 97. [\[CrossRef\]](#)
9. Möderl, M.; Sitzenfrei, R.; Mair, M.; Jarosch, H.; Rauch, W. Identifying Hydropower Potential in Water Distribution Systems of Alpine Regions. In Proceedings of the World Environmental and Water Resources Congress 2012, Albuquerque, NM, USA, 20–24 May 2012; pp. 3137–3146. [\[CrossRef\]](#)
10. Meirelles Lima, G.; Brentan, B.M.; Luvizotto, E. Optimal design of water supply networks using an energy recovery approach. *Renew. Energy* **2018**, *117*, 404–413. [\[CrossRef\]](#)
11. Pugliese, F.; Paola, F.D.; Fontana, N.; Marini, G.; Giugni, M. Small-Scale Hydropower Generation in Water Distribution Networks by Using Pumps as Turbines. *Proceedings* **2018**, *2*, 1486. [\[CrossRef\]](#)
12. Carravetta, A.; Fecarotta, O.; Sinagra, M.; Tucciarelli, T. Cost-Benefit Analysis for Hydropower Production in Water Distribution Networks by a Pump as Turbine. *J. Water Resour. Plan. Manag.* **2014**, *140*, 04014002. [\[CrossRef\]](#)
13. Hamlehdar, M.; Yousefi, H.; Noorollahi, Y.; Mohammadi, M. Energy recovery from water distribution networks using micro hydropower: A case study in Iran. *Energy* **2022**, *252*, 124024. [\[CrossRef\]](#)
14. Latifi, M.; Kerachian, R.; Beig Zali, R. Evaluating energy harvesting from water distribution networks using combined stakeholder and social network analysis. *Energy Strateg. Rev.* **2023**, *49*, 101158. [\[CrossRef\]](#)
15. Amiri-Ardakani, Y.; Najafzadeh, M. Pipe Break Rate Assessment While Considering Physical and Operational Factors: A Methodology based on Global Positioning System and Data-Driven Techniques. *Water Resour. Manag.* **2021**, *35*, 3703–3720. [\[CrossRef\]](#)
16. Zeidan, M.; Ostfeld, A. Hydraulic Ram Pump Integration into Water Distribution Systems for Energy Recovery Application. *Water* **2021**, *14*, 21. [\[CrossRef\]](#)
17. Ramos, H.M.; Morani, M.C.; Pugliese, F.; Fecarotta, O. Integrated Smart Management in WDN: Methodology and Application. *Water* **2023**, *15*, 1217. [\[CrossRef\]](#)
18. Monteiro, L.; Delgado, J.; Covas, D. Improved Assessment of Energy Recovery Potential in Water Supply Systems with High Demand Variation. *Water* **2018**, *10*, 773. [\[CrossRef\]](#)
19. Loots, I.; van Dijk, M.; van Vuuren, S.J.; Bhagwan, J.N.; Kurtz, A. Conduit-hydropower potential in the City of Tshwane water distribution system: A discussion of potential applications, financial and other benefits. *J. S. Afr. Inst. Civ. Eng.* **2014**, *56*, 2–13.
20. Samora, I.; Manso, P.; Franca, M.J.; Schleiss, A.J.; Ramos, H.M. Opportunity and Economic Feasibility of Inline Microhydropower Units in Water Supply Networks. *J. Water Resour. Plan. Manag.* **2016**, *142*, 04016052. [\[CrossRef\]](#)
21. de Marinis, G.; Granata, F.; Santopietro, S.; Savić, D.; Kapelan, Z.; Gargano, R.; Morley, M.S.; Tricarico, C. Optimal energy recovery by means of pumps as turbines (PATs) for improved WDS management. *Water Supply* **2018**, *18*, 1365–1374. [\[CrossRef\]](#)
22. Moazeni, F.; Khazaei, J. Optimal energy management of water-energy networks via optimal placement of pumps-as-turbines and demand response through water storage tanks. *Appl. Energy* **2021**, *283*, 116335. [\[CrossRef\]](#)
23. Sambito, M.; Piazza, S.; Freni, G. Stochastic Approach for Optimal Positioning of Pumps As Turbines (PATs). *Sustainability* **2021**, *13*, 12318. [\[CrossRef\]](#)
24. Brady, J.; Gallagher, J.; Corcoran, L.; Coughlan, P.; McNabola, A. Effects of Long-Term Flow Variation on Microhydropower Energy Production in Pressure Reducing Valves in Water Distribution Networks. *J. Water Resour. Plan. Manag.* **2017**, *143*, 04016076. [\[CrossRef\]](#)
25. Fontana, N.; Giugni, M.; Glielmo, L.; Marini, G.; Zollo, R. Operation of a Prototype for Real Time Control of Pressure and Hydropower Generation in Water Distribution Networks. *Water Resour. Manag.* **2018**, *33*, 697–712. [\[CrossRef\]](#)
26. Creaco, E.; Galuppini, G.; Campisano, A. Unsteady flow modelling of hydraulic and electrical RTC of PATs for hydropower generation and service pressure regulation in WDN. *Urban Water J.* **2021**, *19*, 233–243. [\[CrossRef\]](#)

27. Fontana, N.; Marini, G.; Creaco, E. Comparison of PAT Installation Layouts for Energy Recovery from Water Distribution Networks. *J. Water Resour. Plan. Manag.* **2021**, *147*, 04021083. [[CrossRef](#)]
28. Le Marre, M.; Mandin, P.; Lanoisellé, J.-L.; Zilliox, E.; Rammal, F.; Kim, M.; Inguanta, R. Pumps as turbines regulation study through a decision-support algorithm. *Renew. Energy* **2022**, *194*, 561–570. [[CrossRef](#)]
29. Sitzenfrei, R.; von Leon, J. Long-time simulation of water distribution systems for the design of small hydropower systems. *Renew. Energy* **2014**, *72*, 182–187. [[CrossRef](#)]
30. Sitzenfrei, R.; von Leon, J.; Rauch, W. Design and Optimization of Small Hydropower Systems in Water Distribution Networks Based on 10-Years Simulation with Epanet2. *Procedia Eng.* **2014**, *89*, 533–539. [[CrossRef](#)]
31. Metropolis, N.; Ulam, S. The Monte Carlo Method. *J. Am. Stat. Assoc.* **1949**, *44*, 335–341. [[CrossRef](#)]
32. Sitzenfrei, R.; Rauch, W. Optimizing Small Hydropower Systems in Water Distribution Systems Based on Long-Time-Series Simulation and Future Scenarios. *J. Water Resour. Plan. Manag.* **2015**, *141*, 04015021. [[CrossRef](#)]
33. Hagberg, A.; Swart, P.; Chult, S.D. *Exploring Network Structure, Dynamics, and Function Using NetworkX*; Los Alamos National Lab. (LANL): Los Alamos, NM, USA, 2008.
34. Rossman, L.A.; Woo, H.; Tryby, M.; Shang, F.; Janke, R.; Haxton, T. *EPANET 2.2 User Manual*; Water Infrastructure Division, Center for Environmental Solutions and Emergency Response; U.S. Environmental Protection Agency: Cincinnati, OH, USA, 2020.

Disclaimer/Publisher’s Note: The statements, opinions and data contained in all publications are solely those of the individual author(s) and contributor(s) and not of MDPI and/or the editor(s). MDPI and/or the editor(s) disclaim responsibility for any injury to people or property resulting from any ideas, methods, instructions or products referred to in the content.